

# Hybrid Materials Covalently Incorporated with Isophorone-Based Dyes through Sol–Gel Process for Nonlinear Optical Applications

Lujian Chen, Guodong Qian,\* Yuanjing Cui, Xuefeng Jin, Zhiyu Wang, and Minquan Wang

Department of Materials Science and Engineering, State Key Lab of Silicon Materials, Zhejiang University, Hangzhou 310027, People's Republic of China

Received: June 19, 2006; In Final Form: August 4, 2006

Two new push–pull type second-order nonlinear optical (NLO) active isophorone-based alkoxysilane dyes with the same acceptor were synthesized and characterized. One silane (ICTES-HEMA) bears a chromophore with a hydroxyethyl methylamino donor and the other silane (ICTES-HMPP) is a bulkier analogue with a hydroxymethyl diphenylamino donor. Transparent, homogeneous films were prepared via the copolymerization of tetraalkoxysilane (TEOS) and different NLO silanes with the ratio of 5:1. The  $d_{33}$  values obtained for the HEMA and HMPP films are 46.3 and 20.6 pm/V, respectively. Normalized UV–vis spectra reveal that the introduction of a diaryl group would help to prevent unfavorable organization of the chromophores. The reorientation dynamic stabilities of the samples were studied by second-harmonic generation (SHG) measurements, demonstrating that bulkier chromophores incorporated in sol–gel materials would not necessarily lead to higher stabilities over time.

## Introduction

Over the past decade, significant interests have been generated for developing organic and organomineral hybrid electrooptic (EO) polymers incorporated with nonlinear optical (NLO) chromophores,<sup>1,2</sup> due to their potential applications including optical data transmission and optical information processing.<sup>3,4</sup> To prevent the relaxation of dipolar NLO dyes in amorphous host once they are aligned by the poling process, the NLO chromophores should be covalently attached to the polymer backbone. When a covalent bond is formed between the NLO chromophores and the host, phase separation and the sublimation of chromophores under poling can almost be obviated. A great deal of progress has been made in producing more stable poled polymer systems.<sup>2,5</sup> Sol–gel derived hybrid polymers have been rightfully described as a highly promising alternative and versatile synthetic approach to the fabrication of amorphous three-dimensional optical networks.<sup>6</sup> In this strategy, the design and synthesis of new network-forming alkoxysilane dye are of paramount importance and detailed investigations on them will offer a great promise in the fabrication of new materials for second-order nonlinear optics, which will eventually meet the basic requirements in building photonic devices

Organic molecules with high hyperpolarizabilities ( $\beta$ ) have diverse and important technical issues. Attention has been essentially focused on dipolar molecules for several decades in the quest for improving NLO properties.<sup>7–9</sup> Recent progresses include the exploration of long-conjugated isophorone-based chromophores (i.e. CLD series), which exhibit high  $\beta$  values, and the EO devices based on them show commercial promise.<sup>8,9</sup> Azobenzene dyes were conveniently used to be covalently incorporated in hybrid films due to the ease of synthesis and purification, but the inherent  $\beta$  value is limited.<sup>10</sup> Furthermore, there were few reports on newly synthesized isophorone-based

alkoxysilane dyes. Little information of sol–gel systems with isophorone-based chromophores was described.

The research in chromophores design seems to be shifting to the optimization of the hyperpolarizability and a variety of other parameters, i.e., thermal stability, chemical stability and optical loss.<sup>11</sup> To study the sol–gel films covalently incorporated with isophorone-based dyes, the strategy was adopted as discussed below for comparison: the diarylamino donor was substituted for a dialkylamino donor to build a bulkier structure, which can also improve the thermal stability of the chromophore without a major compromise in optical nonlinearities, as shown in previous reports.<sup>11–13,25</sup> Then the NLO chromophore is covalently attached to a polymerizable silane to yield a precursor which can be copolymerized with tetraalkoxysilane (TEOS) under sol–gel hydrolysis/condensation processing conditions to yield a hybrid material. The molecular structures of the alkoxysilane dyes are shown in Figure 1. Both of the push–pull type dyes and corresponding alkoxysilane precursors were characterized by <sup>1</sup>H NMR and FTIR, etc. Second-harmonic generation (SHG) experiment was used to study the sol–gel films. The results reveal that the introduction of the diarylamino group would help to prevent unfavorable organization of dipolar NLO molecules, but the incorporation of a bulkier chromophore in a sol–gel material would not necessarily lead to more stable nonlinearities over time.

## Experimental Part

**Materials.** All starting materials were purchased from Acros Organics, Fluka, Alfa Aesar, TCI, or Aldrich and were used without further purifications. Tetrahydrofuran (THF) was dried by refluxing, distilling from calcium hydride just before use. Other solvents, of analytical-grade quality, were commercial products and used as received.

**Synthesis of 2-(3,5,5-Trimethylcyclohex-2-enylidene)malononitrile (1).** A solution of isophorone (16.5 mL, 110 mmol), malononitrile (6.6 g, 100 mmol), piperidine (1.8 mL, 18.2

\* To whom correspondence should be addressed. Tel.: +86-571-87952334. Fax: +86-571-87951234. E-mail: gdqian@zju.edu.cn.

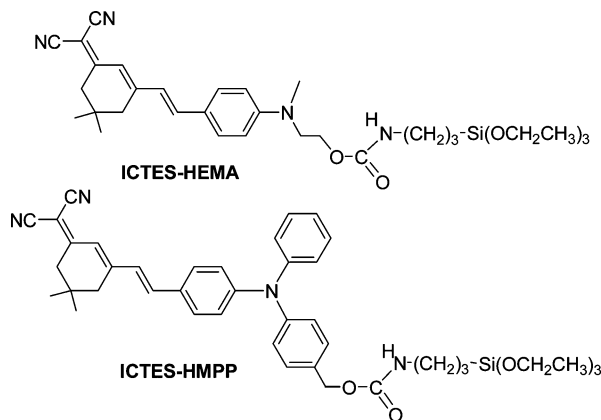


**Figure 1.** Chemical structures of alkoxyisilane dyes investigated in this study.

mmol), glacial acetic acid (0.40 mL, 7.0 mmol), and acetic anhydride (0.2 g, 2.0 mmol) in dimethylformamide (DMF; 55 mL) was stirred at room temperature for 6 h and then refluxed at 120 °C for 6 h under nitrogen atmosphere. After being cooled to room temperature, the reaction mixture was poured into water. The crude products were collected and washed with brine; then the residue was purified by column chromatography (silicagel) using petroleum ether/ethyl acetate (12/1, v/v) as eluent. Pale-yellow solids were obtained. Yield: 53%.  $^1\text{H}$  NMR (500 MHz,  $\text{CDCl}_3$ , ppm):  $\delta$  1.04 (s, 6H,  $\text{CH}_2(\text{CH}_3)_2\text{CH}_2$ ), 2.05 (s, 3H,  $\text{CH}_3$ ), 2.20 (s, 2H,  $\text{CH}_2(\text{CH}_3)_2\text{CH}_2$ ), 2.54 (s, 2H,  $\text{CH}_2(\text{CH}_3)_2\text{CH}_2$ ), 6.64 (s, 1H,  $\text{CH}=\text{C}$ ). Anal. Calcd for  $\text{C}_{12}\text{H}_{14}\text{N}_2$  (186.25): C, 77.38; H, 7.58; N, 15.04. Found: C, 77.26; H, 7.68; N, 15.00.

**Synthesis of 4-((2-Hydroxyethyl)methylamino)benzaldehyde (2).** To a solution of 12.8 g of 2-(methylamino)ethanol, 5.96 g of 4-fluorobenzaldehyde, a catalysis amount of 18-crown-6 in 12 mL of dimethyl sulfoxide (DMSO), and 10 g of anhydrous potassium carbonate were added. The mixture is heated at 95 °C for 3 days. The product mixture is cooled and poured into ice water. The resultant solid precipitate is filtered, washed with water, and purified by column chromatography (silica gel) using petroleum ether/ethyl acetate (4/1, v/v) as eluent. Pale-yellow solids were obtained. Yield: 61%.  $^1\text{H}$  NMR (500 MHz,  $\text{CDCl}_3$ , ppm):  $\delta$  2.04 (s, 3H,  $\text{NCH}_2\text{CH}_2\text{OH}$ ), 3.13 (s, 3H,  $\text{CH}_3$ ), 3.62–3.64 (t, 2H,  $\text{CH}_2\text{CH}_2\text{OH}$ ), 3.87–3.89 (t, 2H,  $\text{CH}_2\text{CH}_2\text{OH}$ ), 6.77–6.79 (d, 2H, ArH), 7.71–7.72 (d, 2H, ArH), 9.71 (s, 1H, CHO). Anal. Calcd for  $\text{C}_{10}\text{H}_{13}\text{NO}_2$  (179.09): C, 67.02; H, 7.31; N, 7.82. Found: C, 65.90; H, 7.28; N, 7.91.

**Synthesis of 4,4'-(Phenylazanediyl)dibenzaldehyde (3).** To 16.5 mL (180 mmol) of  $\text{POCl}_3$  in an ice bath, an equal molar amount of DMF (13.8 g) was added dropwise with vigorous stirring for 0.5 h to form a Vilsmeier reagent. Then 10 g (40 mmol) of triphenylamine was added, followed by stirring at 85 °C under  $\text{N}_2$  atmosphere for 12 h, cooled, and then poured into ice water slowly. The mixture was then neutralized with 10% NaOH solution, extracted by dichloromethane, filtered, washed with water, and dried. After evaporation of dichloromethane, the dark-green oil was first purified by column chromatography (neutral alumina) using toluene as eluent. After evaporation of the solvent the remaining reaction product was recrystallized from toluene/petroleum ether for three times to give yellow crystals. Yield: 63%.  $^1\text{H}$  NMR (500 MHz,  $\text{CDCl}_3$ , ppm):  $\delta$  7.17–7.19 (m, 6H, ArH), 7.25–7.28 (t, 1H, ArH), 7.38–7.41 (t, 2H, ArH), 7.76–7.78 (d, 4H, ArH), 9.89 (s, 2H, CHO). Anal. Calcd for  $\text{C}_{20}\text{H}_{15}\text{NO}_2$  (301.34): C, 79.72; H, 5.02; N, 4.65. Found: C, 79.65; H, 5.07; N, 4.75.

**Synthesis of 4-((4-(Hydroxymethyl)phenyl)phenylamino)-benzaldehyde (4).** To a solution of 4 g (13.28 mmol) of 4,4'-(phenylazanediyl)dibenzaldehyde (2) in 25 mL of dry THF, 128 mg (0.16 mmol) of sodium borohydride in 8 mL of ethanol was added dropwise under stirring. After stirring for 1.5 h at room temperature, the reaction mixture was neutralized with diluted hydrochloric acid and extracted with dichloromethane. The extract was washed out with water and dried. After filtration, the solvent was evaporated and the residue was purified by column chromatography (silica gel) using petroleum ether/ethyl acetate (4/1, v/v) as eluent. Light yellow oil was obtained. Yield: 72%.  $^1\text{H}$  NMR (500 MHz,  $\text{CDCl}_3$ , ppm):  $\delta$  1.85 (s, 1H,  $-\text{Ph}-\text{CH}_2-\text{OH}$ ), 4.69 (s, 2H,  $-\text{Ph}-\text{CH}_2-\text{OH}$ ), 7.15–7.18 (t, 5H, ArH), 7.32–7.35 (t, 4H, ArH), 7.66–7.68 (d, 2H, ArH), 9.80 (s, 1H, CHO).

**Synthesis of 2-(3-(4-((2-Hydroxyethyl)methylamino)styryl)-5,5-dimethylcyclohex-2-enylidene)malononitrile (HEMA).** A mixture of 4.65 g (26 mmol) of 4-((2-hydroxyethyl)methylamino)benzaldehyde (2), 6 g of (32 mmol) of **1**, 4 mL of piperidine, 2 mL of acetic acid, and 2 mL of acetic anhydride in 20 mL of DMF was stirred at 80 °C for 8 h. After cooling, the reaction mixture was poured into iced water (200 mL). The precipitate was filtered, washed with water, and air-dried and then purified by column chromatography (silica gel) using petroleum ether/ethyl acetate (1/2, v/v) as eluent. HEMA was obtained as dark red crystals. Yield: 78%. Mp: 162.1 °C.  $^1\text{H}$  NMR (500 MHz,  $\text{CDCl}_3$ , ppm):  $\delta$  1.01 (s, 6H,  $\text{CH}_2(\text{CH}_3)_2\text{CH}_2$ ), 2.05 (s, 1H,  $\text{CH}_2\text{CH}_2\text{OH}$ ), 2.45 (s, 2H,  $\text{CH}_2(\text{CH}_3)_2\text{CH}_2$ ), 2.57 (s, 2H,  $\text{CH}_2(\text{CH}_3)_2\text{CH}_2$ ), 3.09 (s, 3H,  $\text{NCH}_3$ ), 3.57–3.59 (t, 2H,  $\text{CH}_2\text{CH}_2\text{OH}$ ), 3.87 (s, 2H,  $\text{CH}_2\text{CH}_2\text{OH}$ ), 6.75–6.79 (m, 3H, ArH,  $\text{CH}=\text{C}$ ), 6.78–6.79 (d, 1H,  $\text{CH}=\text{CH}$ ,  $J = 16$ ), 7.00–7.03 (d, 1H,  $\text{CH}=\text{CH}$ ,  $J = 16$ ), 7.40–7.42 (d, 2H, ArH). Anal. Calcd for  $\text{C}_{21}\text{H}_{23}\text{N}_3\text{O}$  (333.18): C, 75.65; H, 6.95; N, 12.60. Found: C, 74.99; H, 6.90; N, 11.64.

**Synthesis of 2-(3-(4-((4-(Hydroxymethyl)phenyl)phenylamino)styryl)-5,5-dimethylcyclohex-2-enylidene)malononitrile (HMPP).** To a solution of 2.4 g (7.9 mmol) of 4-((4-(hydroxymethyl)phenyl)phenylamino)benzaldehyde (4) and 1.47 g (7.9 mmol) of **1** in 10 mL of DMF, 2 mL of acetic acid, 2 mL of piperidine, and 1 mL of acetic anhydride were added. The reaction mixture was heated at 80 °C for 8 h under stirring, cooled, and poured into water. After filtration the crude reaction product was purified first by column chromatography onto silica gel using dichloromethane/ethyl acetate (4/1, v/v) as eluent. After evaporation of the solvent the remaining reaction product was recrystallized from ethanol to obtain the pure product. Yield: 62%. Mp: 183.1 °C.  $^1\text{H}$  NMR (500 MHz,  $\text{DMSO}-d_6$ , ppm):  $\delta$  1.01 (s, 6H,  $\text{CH}_2(\text{CH}_3)_2\text{CH}_2$ ), 2.53 (s, 2H,  $\text{CH}_2(\text{CH}_3)_2\text{CH}_2$ ), 2.60 (s, 2H,  $\text{CH}_2(\text{CH}_3)_2\text{CH}_2$ ), 4.47–4.48 (t, 2H,  $\text{NArCH}_2\text{O}$ ), 5.16–5.19 (t, 1H,  $\text{NArCH}_2\text{OH}$ ), 6.81 (s, 1H), 6.86–6.87 (d, 2H), 7.05–7.09 (m, 4H), 7.12 (t, 1H), 7.30–7.37 (m, 4H), 7.57–7.58 (d, 1H). Anal. Calcd for  $\text{C}_{32}\text{H}_{29}\text{N}_3\text{O}$  (471.23): C, 81.50; H, 6.20; N, 8.91. Found: C, 80.91; H, 6.26; N, 8.66.

**Synthesis of Alkoxyisilane Dyes. General Procedure.** A dry, 50 mL three-necked flask equipped with an oil bath, a mechanical stirrer, a nitrogen inlet, and a reflux condenser was charged with 4 mmol of chromophore, 3-isocyanatopropyltriethoxysilane (ICTES, 1.19 g, 4.8 mmol), 15 mL of THF, and 5 drops of triethylamine (TEA) as catalyst. The reaction mixture was stirred and refluxed for 48 h under nitrogen atmosphere. The resulting alkoxyisilane dye was purified by flash column chromatography onto silica gel using petroleum ether/ethyl acetate (1/1, v/v) as eluent.

**ICTES-HEMA.** Yield: 65%.  $^1\text{H}$  NMR (500 MHz,  $\text{DMSO}-d_6$ , ppm):  $\delta$  0.49–0.52 (t, 2H,  $\text{CH}_2\text{CH}_2\text{CH}_2$ ), 1.01 (s, 6H,  $\text{CH}_2-(\text{CH}_3)_2\text{CH}_2$ ), 1.12–1.15 (t, 9H,  $\text{CH}_2\text{CH}_3$ ), 1.41–1.44 (t, 2H,  $\text{CH}_2\text{CH}_2\text{CH}_2$ ), 2.54 (s, 2H,  $\text{CH}_2(\text{CH}_3)_2\text{CH}_2$ ), 2.58 (s, 2H,  $\text{CH}_2-(\text{CH}_3)_2\text{CH}_2$ ), 2.92–2.94 (d, 2H,  $\text{CH}_2\text{CH}_2\text{CH}_2$ ), 3.00 (s, 3H,  $\text{NCH}_3$ ), 3.60–3.62 (t, 2H,  $\text{NCH}_2\text{CH}_2\text{O}$ ), 3.71–3.75 (m, 6H,  $\text{CH}_2\text{CH}_3$ ), 4.08–4.10 (t, 2H,  $\text{NCH}_2\text{CH}_2\text{O}$ ), 6.75–6.76 (d, 3H), 7.11–7.14 (d, 1H,  $\text{CH}=\text{CH}$ ,  $J = 16$ ), 7.14–7.16 (m, 1H,  $\text{CH}=\text{C}$ ), 7.22–7.25 (d, 1H,  $\text{CH}=\text{CH}$ ,  $J = 16$ ), 7.53–7.55 (d, 2H,  $\text{ArH}$ ).

**ICTES-HMPP.** Yield: 45%.  $^1\text{H}$  NMR (500 MHz,  $\text{DMSO}-d_6$ , ppm):  $\delta$  0.51–0.54 (t, 2H,  $\text{CH}_2\text{CH}_2\text{CH}_2$ ), 1.01 (s, 6H,  $\text{CH}_2-(\text{CH}_3)_2\text{CH}_2$ ), 1.12–1.15 (m, 9H,  $\text{CH}_2\text{CH}_3$ ), 1.43–1.47 (t, 2H,  $\text{CH}_2\text{CH}_2\text{CH}_2$ ), 2.53 (s, 2H,  $\text{CH}_2(\text{CH}_3)_2\text{CH}_2$ ), 2.60 (s, 2H,  $\text{CH}_2(\text{CH}_3)_2\text{CH}_2$ ), 2.95–2.99 (m, 2H,  $\text{CH}_2\text{CH}_2\text{CH}_2$ ), 3.71–3.75 (m, 6H,  $\text{CH}_2\text{CH}_3$ ), 4.97 (s, 2H,  $\text{NArCH}_2\text{O}$ ), 6.81 (s, 1H), 6.88–6.90 (d, 2H), 7.05–7.09 (m, 4H), 7.13–7.15 (m, 1H), 7.24–7.28 (t, 3H), 7.31–7.38 (m, 4H), 7.58–7.60 (d, 2H).

**Film Preparation.** To prepare the coating solution, each of the alkoxysilane dyes was mixed with TEOS with a molar ratio of 1:5 in THF. Then acidic water ( $\text{HCl}$ ,  $\text{pH} = 1$ ) was added to favor the hydrolysis/condensation process; the  $\text{H}_2\text{O}:\text{Si}$  molar ratio was 4:1. The solution was stirred at room temperature for 6 h and aged for 7 days to increase viscosity. The sol was filtered through a 0.22  $\mu\text{m}$  Teflon membrane filter before spin coating on the indium–tin oxide (ITO) glass substrates. The coated films were dried in a vacuum oven at 80  $^\circ\text{C}$  for 2 h to remove the residual solvent.

**Second-Harmonic Generation Measurement.** The second-order optical nonlinearity of hybrid films was determined by in situ SHG measurement. A closed temperature-controlled oven having optical windows and equipped with tungsten needle electrodes was used. The film, which kept at 45 $^\circ$  to the incident beam, was poled inside the oven. The poling condition was as follows: voltage, 4.5 KV; gap distance, 1 cm. The laser source is a Q-switched Nd:YAG pulse laser with a 1064 nm fundamental beam (500 mJ maximum energy, 3–5 ns pulse width, and 10 Hz repeating rate). The generated second-harmonic wave was passed through a monochromator and detected by a photomultiplier. The signal was averaged on a Stanford Research Systems (SRS) model SR-250 gated integrator and boxcar averager module and transferred to a microcomputer through a computer interface module SR-254.

**Characterization.** Elemental analysis was carried out on an Eager 300 microelemental analyzer.  $^1\text{H}$  NMR spectra were obtained with a Bruker Avance DMX500 spectrometer using tetramethylsilane (TMS) as an internal standard. FTIR spectra were recorded on a Nicolet Avatar 360 in the region of 400–4000  $\text{cm}^{-1}$  using KBr pellets. UV–vis absorption spectroscopic study was performed with a Perkin-Elmer Lambda 20 spectrophotometer. The decomposition temperature was studied using a TA Instruments SDT Q600 at a heating rate of 10  $^\circ\text{C}/\text{min}$  in nitrogen atmosphere. The thickness of thin films was determined using the Metricon PC 2010 prism coupler.

## Results and Discussion

**Synthesis and Characterization.** The multistep synthesis routes of various alkoxysilane dyes are shown in Scheme 1. The preparation sequence of HEMA was an Ullmann coupling followed by a Knoevenagel condensation.<sup>14</sup> HMPP was synthesized via Vilsmeier–Haack formylation, selective reduction of one aldehyde group, and Knoevenagel condensation.<sup>15</sup>

The alkoxysilane dyes ICTES-HEMA and ICTES-HMPP were obtained with acceptable yields through a coupling reaction

between the ICTES and corresponding dyes. Alkoxysilane dyes after coupling reaction were always used directly for sol–gel reaction without further purification.<sup>16</sup> So few experimental data of alkoxysilane dye synthesized were reported previously. Ordinarily, the thermally unstable alkoxysilane dye was purified by a simple dissolve–precipitate procedure at room temperature.<sup>17</sup> So alkoxysilane dyes with low melting point cannot be obtained. Because the weak lines assigned to  $\text{CH}_3$  and  $\text{CH}_2$  from the presence of a small amount of ethanol were found at 1.25 and 3.72 ppm in the  $^1\text{H}$  NMR spectrum,<sup>18</sup> thus confirming the partial hydrolysis of ethoxy groups of purified ICTES-HEMA and ICTES-HMPP,<sup>19</sup> the flash column chromatography was useful to purify alkoxysilane dyes, even those with low melting point.

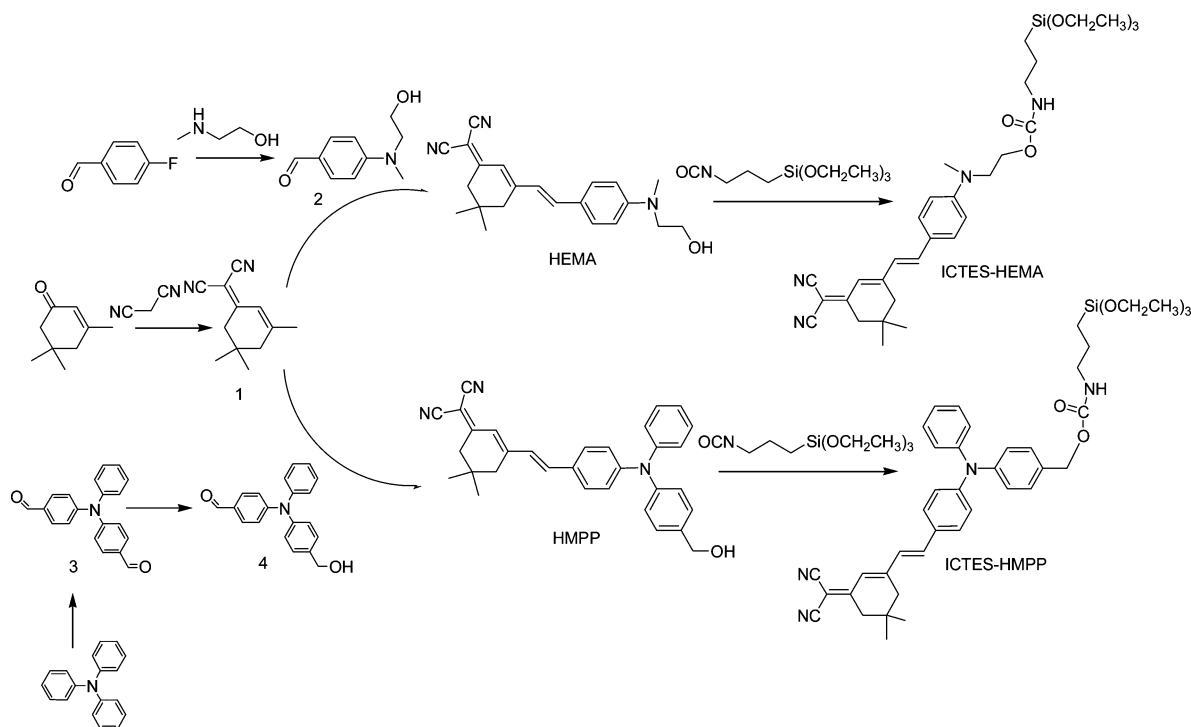
Figure 2 shows FTIR spectra of HEMA, HMPP, and the corresponding alkoxysilanes. For all of them, the C–H stretching vibration of  $\text{CH}_2$  and  $\text{CH}=\text{CH}$  was observed around 2880, 2920, 2950, and 3030  $\text{cm}^{-1}$ . In the spectra of HEMA and HMPP, the absorption corresponding to the hydroxyl was observed at 3510 and 3580  $\text{cm}^{-1}$ . Both of the FTIR spectra reveal the sharp absorption peak corresponding to CN stretching observed at 2210  $\text{cm}^{-1}$ . In addition, the C=C stretching of phenylene was observed at 1600 and 1550  $\text{cm}^{-1}$ . The elemental analysis values of the compounds are generally in good agreement with the calculated values for the proposed structures, indicating that HEMA and HMPP were successfully synthesized. In the spectra of ICTES-HEMA and ICTES-HMPP, the absorption bands at 3410 and 1720  $\text{cm}^{-1}$  emerge, contributed to the urethane group vibrations ( $\gamma_{\text{N-H}}$  and  $\gamma_{\text{C=O}}$ , respectively). The Si–O–C $_2\text{H}_5$  stretching frequencies of alkoxysilane were found at 1070  $\text{cm}^{-1}$ . No band at 2273  $\text{cm}^{-1}$  characteristic of the isocyanate group ( $\gamma_{\text{C=N}}$ ) stretching in ICTES was detected.<sup>17</sup> These results showed that the corresponding alkoxysilanes were obtained.

The decomposition temperatures ( $T_d$ ) of HEMA, HMPP, and DR 1 (obtained from Aldrich) are defined by the onset of the TGA curves as shown in Figure 3, being 299.6 (HEMA), 306.2 (HMPP), and 252.1  $^\circ\text{C}$  (DR1 for comparison). It revealed that HMPP with a diaryl donor has the best thermal stability. Both of the chromophores (HEMA and HMPP) with the same isophorone-based electron-withdrawing group showed increased thermal stability, compared with the traditional azobenzene dye (e.g. DR1), due to the ring-locked isophorone bridge.<sup>8,9,12</sup> The substitution of the hydroxymethyl diphenylamino group for a hydroxyethyl methylamino group could also lead to the improvement of thermal stabilities.<sup>11–13</sup>

Transparent and stable inorganic–organic hybrid films were prepared through the hydrolysis and copolymerization process of different dye-bonded precursors with TEOS. The thicknesses of the films were in the range of 0.3–0.5  $\mu\text{m}$ . TEOS was used as a cross-linking reagent to increase the network rigidity. The spin-coated hybrid films are tough and resistant to organic solvents. No measurable concentration of the dyes from the vacuum-dried films was extracted by THF, which is a good solvent for the alkoxysilane dyes, suggesting that the chromophores have been firmly incorporated into the silica matrix. An appropriate amount of sol solution was poured on the glass, allowed to gel, and then cured for 12 h at 140  $^\circ\text{C}$ , which corresponds to the poling temperature. After thermal curing, the gels were ground with KBr and pressed into pellets to perform structural characterization by FTIR. The absorption band characterized for the vibration of the urethane group ( $\gamma_{\text{C=O}} = 1720 \text{ cm}^{-1}$ ) was observed in all FTIR spectra, showing



## SCHEME 1: Synthesis Route of the Alkoxysilane Dyes



that the bond between the siloxane network and the dye had been conserved upon thermal curing.

In the FTIR spectra of gels presented in Figure 4, a large absorption band between 1200 and 1000  $\text{cm}^{-1}$  due to the Si—O—Si stretching was observed, illustrating that the dye-attached precursor has hydrolyzed and polymerized. This band has several components which reveal the presence of species with different structure and symmetry. T notation usually refers to the oxo trifunctional  $\text{R}'\text{—SiO}_3$  central unit. According to a previously reported analysis,<sup>19</sup> the absorption bands characteristic of the  $\gamma(\text{Si—O—Si})_{\text{asym}}$  vibrations could be split into two main components located at 1050 and 1120  $\text{cm}^{-1}$  assigned to T linear polysiloxane structures and T cyclic caged ones, respectively. The analysis of the intensities of the two main  $\gamma(\text{Si—O—Si})$  components shows that the thermal curing renders both of the hybrid siloxane—oxide structures more linear. Moreover, the feature around 950  $\text{cm}^{-1}$  attributed to the Si—OH bond is revealed and shows a decrease after the thermal treatment.

**Linear Optical Properties.** Normalized UV—vis absorption spectra of HEMA and HMPP in THF and in sol—gel films are shown in Figure 5. The maximum absorption wavelengths ( $\lambda_{\text{max}}$ ) of HEMA and HMPP in THF appear at 507 and 492 nm, respectively, due to intramolecular charge transfer (ICT). Obviously, HEMA shows lower energy of the visible low-energy charge-transfer absorptions than HMPP. Measurement of the electron-transfer (ET)-donor strength by calculation of vertical ionization potentials (IPs) shows that triarylamines are more readily ionized than their *N,N*-dialkylanilines analogues.<sup>20</sup> Despite the parent triphenylamine being a better ET-donor than *N,N*-dialkylaniline, the 4-(diphenylamino)phenyl group is clearly seen to be a poorer  $\pi$ -donor in HMPP than the 4-(dimethylamino)phenyl group in HEMA. This difference in  $\pi$ -donor strengths is indeed primarily due to the sterically induced twisting effect:<sup>20</sup> in the 4-(diphenylamino)phenyl system there is a dihedral angle,  $\psi$ , of ca. 40° between the plane of the  $\text{C}_6\text{H}_4\text{X}$  ring and the plane formed by the N atom and the two attached carbon atoms of the terminal R groups, whereas the correspond-

ing angle in the 4-(dimethylamino)phenyl system is close to zero. In addition,  $^1\text{H}$  NMR data ( $\delta$  CHO, 9.71) of 2 and  $^1\text{H}$  NMR data ( $\delta$  CHO, 9.80) of 4 are consistent with previous studies,<sup>21</sup> proving stronger  $\pi$ -donor strength provided by the introduction of (dimethylamino)phenyl group.

The maximum absorption wavelength of HEMA in TEOS-based sol—gel material is 25 nm blue-shifted than in THF solvent; i.e., the maximum absorption wavelength is 482 nm for HEMA in the sol—gel film. But HMPP have the same  $\lambda_{\text{max}}$  position in both the sol—gel matrix and in THF solvent (492 nm). Remarkably, HEMA and HMPP have the same acceptor unit and similar dipole moment. It seems reasonable to suspect that the sterical factor have a significant influence on the dye-aggregation induced blue-shift and widening of the absorption band,<sup>22</sup> in addition to the well-known solvatochromic effect of the dipolar nature of the dyes. In other words, the chromophore HMPP with a diaryl group has a quinoidal bonding pattern,<sup>23</sup> which may help to prevent unfavorable organization of the chromophores, making the antiparallel alignment of two nearby molecules less efficient. The results confirm that the replacement of the dialky group with a diaryl group strongly reduces the aggregation of chromophores that would occur at this concentration, which allows achieving higher loadings of chromophores with a good dispersion within the host. It is also noteworthy that the strong conjugation enhancement was observed at 532 nm due to strong absorption intensity.

**Nonlinear Optical Properties.** As we know, when the indirect solvatochromism method was chosen to evaluate  $\beta_{\text{CT}}\mu_{\text{g}}$  values of chromophores, the estimation of an arbitrary “solvent cavity radius” parameter  $\alpha$  is raised to the third power in the determination of hyperpolarizabilities.<sup>24</sup> Given that, the solvent cavity of the diarylamino donor compound must be substantially different at the donor end of the molecule but will be identical at the acceptor end of the molecule. It is hard to imagine that  $\beta$  values sufficient for a valid comparison could be obtained by solvatochromism method. Fortunately, electric field-induced second-harmonic (EFISH) generation experiments on a series of isophorone dyes were performed by Ermer and co-workers

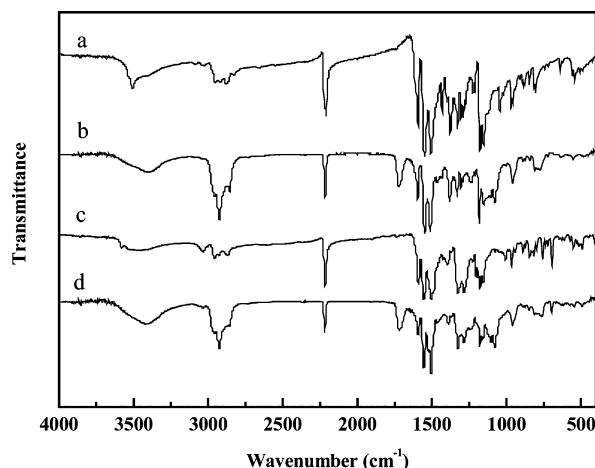


**Figure 2.** FTIR spectra of HEMA (a), ICTES-HEMA (b), HMPP (c), and ICTES-HMPP (d).

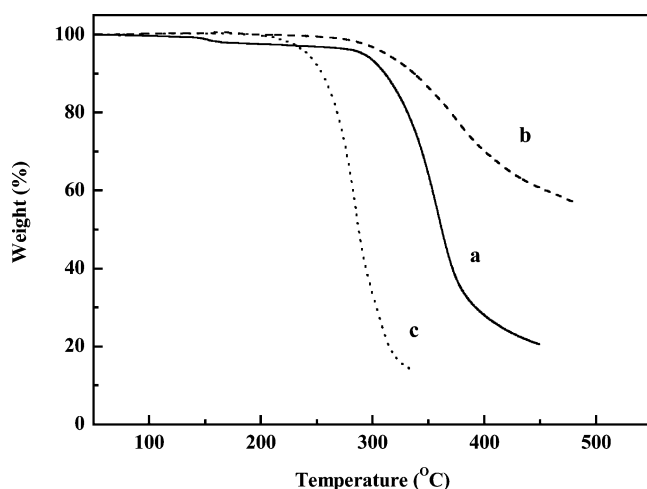


**Figure 3.** TGA traces for chromophore HEMA (a), HMPP (b), and DR1 (c).

in order to determine actual hyperpolarizability.<sup>25</sup> Chromophore HEMA in our study is very similar to the dialkylamino chromophore **1f** of Ermer et al. (as well as **1a** and **1b**), while chromophore HMPP is very similar to the diarylamino compound **1i** of them. We use their numbers and the two-level model of Oudar and Chemla to determine the nonlinearities of our compounds at 1064 nm corresponding to the SHG experiments in our research.<sup>26</sup> The prediction says that HEMA (**1f**) would have a nonlinearity ( $\mu_g\beta_{CT}$ ) of  $1.66 \times 10^{-44}$  esu, while HMPP (**1i**) would have a nonlinearity of  $1.36 \times 10^{-44}$  esu. The dialkylamino compound would be 22% higher, which can be attributed to better  $\pi$ -donor ability of the 4-(dimethylamino)-phenyl system as mentioned above.

The second-order NLO properties of the hybrid films were characterized by SHG measurement using the Maker fringe technique.<sup>27,28</sup> The second-harmonic coefficient ( $d_{33}$ ) of hybrid film can be calculated by comparison with the SHG intensity of a standard Y-cut quartz crystal plate. When the sample absorption was taken into account in our calculations, the  $d_{33}$  values of films containing HEMA and HMPP were obtained to be 46.3 and 20.6 pm/V, respectively. It should be addressed that the HEMA-based material was better than HMPP by a factor of more than 2. The relative nonlinearities of sol–gel films are quite different with the relative nonlinearities of the chromophores alone. Commonly, the NLO properties of the materials include the degree to which the chromophores were successfully oriented within the films by the poling process, which may differ

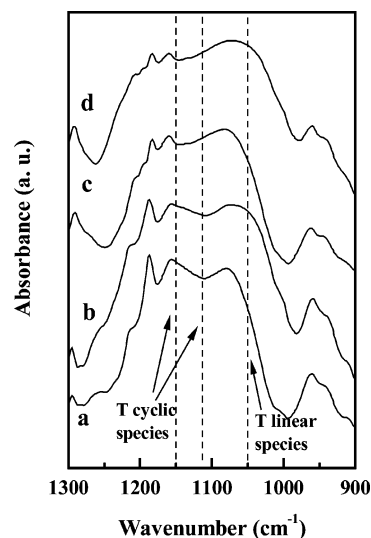


**Figure 4.** FTIR spectra of the sol with HEMA (a), the cured xerogel with HEMA (b), the sol with HMPP (c), and the cured xerogel with HMPP (d).

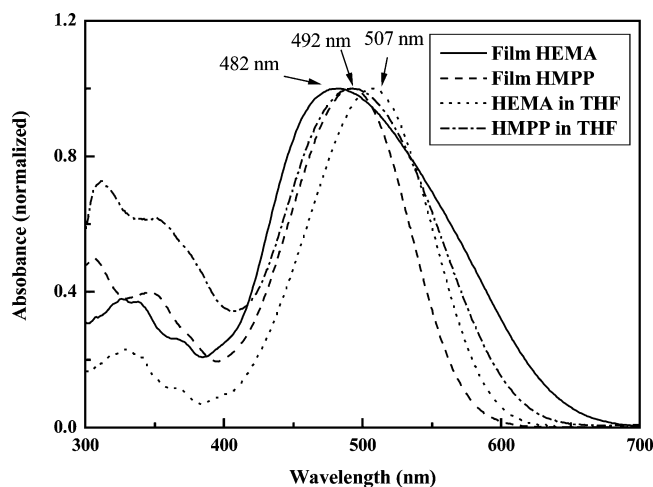


**Figure 5.** Normalized UV–vis absorption spectra of NLO dyes in THF and hybrid film.

between the two materials. Two possible explanations come to mind. First, the bulkier HMPP should be more difficult to pole, which would lead to an even bigger discrepancy between the two materials than was observed for just the chromophores, as we observed in this study. Second, the poling voltage was set at constantly 4.5 kV for different films with different thicknesses. The HEMA-based thin film (with a thickness of 234 nm) could be oriented more effectively than the HMPP-based thicker film (421 nm) and results in an improvement of the NLO coefficient.

**Thermal Dynamic Behavior.** As far as NLO devices are concerned, the thermal stability of the poled films should be optimized to withstand the short-term thermal shock for device processing and packaging. The stability of a poling-induced dipole of two different hybrid materials was studied by thermal depoling experiment. The temperature dependence of the dipolar reorientation of the NLO films can be investigated via monitoring normalized  $d_{33}$  coefficient as a function of temperature. The poled film was heated at a rate of 10 °C/min from 40 to 250 °C. Figure 6 shows the results of the hybrid films containing HEMA and HMPP. Both of the films were poled at 140 °C for 1 h. It can be seen that the half-decay temperatures were about 130 °C for the HEMA-based film and about 120 °C for the HMPP-based film.

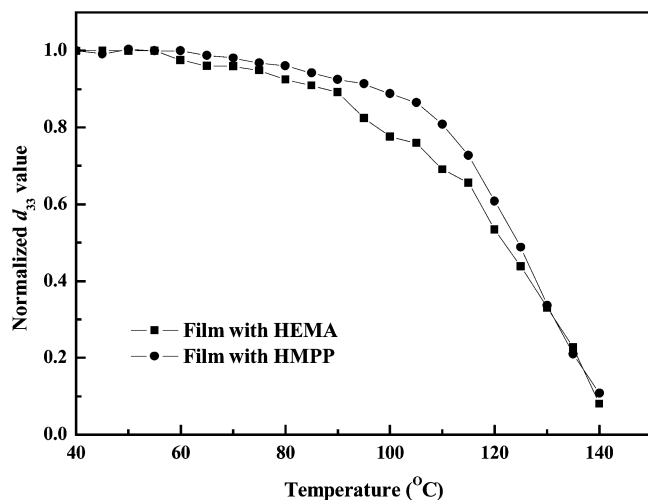


**Figure 6.** Decay of the normalized  $d_{33}$  values as a function of temperature for the films poled at 140 °C for 1 h containing HEMA and HMPP.

In these sol–gel films, the NLO molecule is attached into the silica backbone as a side pendant. Traditionally, the free volume of the network is sufficient to allow reorientation of the chromophores after poling because the size of the siloxane linkage and the propyl chain is large. A chromophore with a long rodlike structure should also result in more stable polymer systems because the rotation of long rodlike side groups at temperatures below  $T_g$  requires a much larger free volume to be made available by the cooperative molecular motions associated with the glass transition.<sup>29</sup> It was reported that the relaxation of small-size dyes such as substituted benzenes and styrenes is much faster than that of large ones such as substituted stilbenes and tolans,<sup>30</sup> just contrary to the situation we found in these sol–gel films. A proper explanation was that bulky diphenyl group located at the donor side of ICTES-HMPP influences the hydrolysis and copolymerization process of the dye-bonded precursor with TEOS. The weak cross-linking efficiency can be due to the dye size.<sup>19</sup> And it has also been reported that the condensation of polyfunctional alkoxy silanes is always difficult to complete.<sup>31</sup> The qualitative comparison between the intensities of the linear and cyclic components in FTIR spectra of sols and xerogels (Figure 4) illustrates the cross-link degree of the siloxane–silica phase. The formation of T cyclic structures was also found to be favored in the sol and xerogel with relatively small-size dye HEMA, leading to a rigid and cross-linked structure which can help to prevent dipolar relaxation.<sup>19</sup>

Among various classes of NLO chromophores, triphenylamine derivatives with a higher decomposition temperature were promising candidates for NLO applications because of their multifunctional properties, such as two-photon absorption and hole-conducting properties.<sup>32</sup> For these reasons, triphenylamine derivatives such as HMPP attract our attention. In addition, it was found that the temporal stabilities of the films with thermoset properties were greatly enhanced when poling time extended and temperature became higher, as shown in Figure 7. The formation of smaller free volumes in rigid inorganic networks would potentially help freeze the chromophore molecules.<sup>33</sup> But the ubiquitous poling bleach effect of chromophores would become pronounced and could not be ignored. To solve the poling bleach problem, a layer of poly(vinyl alcohol) (PVA) should be coated on the film beforehand.<sup>34</sup>

Vertical, parallel, and vertical–parallel systems according to the bonding direction between chromophores and silica matrix

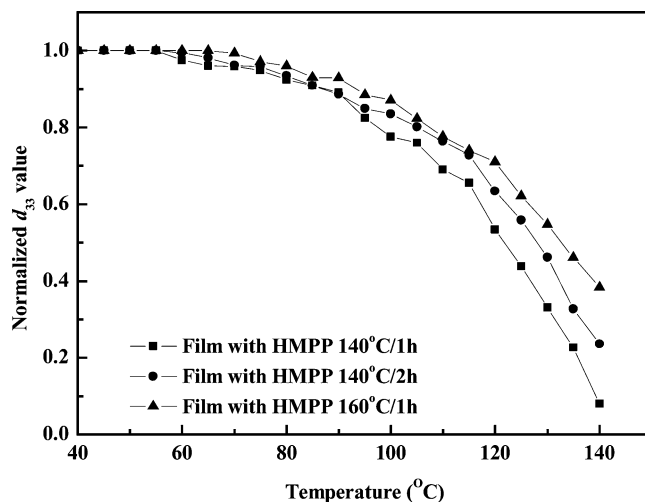


**Figure 7.** Decay of the normalized  $d_{33}$  values as a function of temperature for the films with different poling conditions.

were characterized and studied,<sup>35</sup> displaying that the vertical–parallel system with higher cross-linking sites would have a better stability than the vertical and parallel systems. But only one vertical bonding direction is created in our study, which can explain why the poling stability results are what they are. Recently, Zhang and co-workers have developed a multicomposition cross-linked hybrid sol–gel for nonlinear optic and electrooptic applications.<sup>36</sup> In addition to having rigid inorganic networks, the system also possesses polymerizability and cross-linkability, leading to the high thermal stability. The strategies of developing highly cross-linked systems would be considered in our further research of NLO sol–gel materials with enhanced poling stabilities.

## Conclusion

In conclusion, two new inorganic–organic hybrid films covalently incorporated with dialkylamino- and diarylamino-substituted isophorone-based chromophores were prepared by the sol–gel technique. SHG measurement indicated that the second harmonic coefficients ( $d_{33}$ ) at 1064 nm of hybrid films were 46.3 (HEMA) and 20.6 pm/V (HMPP). UV–vis spectra reveal that the introduction of a diarylamino group could help to prevent unfavorable organizations of the chromophores. Through comparative study of the NLO thermal stability of the sol–gel systems containing HEMA and HMPP, we learned that different hydrolysis and copolymerization processes of silane precursors may have a major influence on the degree of cross-linking of the siloxane–silica phase. As a consequence, a bulkier alkoxy silane dye possessing different sol–gel behaviors would not necessarily lead to more stable nonlinearities over time.

**Acknowledgment.** The authors gratefully acknowledge the financial support for this work from the National Natural Science Foundation of China (under Grant No. 50532030) and the Foundation for the Author of National Excellent Doctoral Dissertation of the People's Republic of China (Grant No. 200134).

## References and Notes

- (1) Marder, S. R.; Kippelen, B.; Jen, A. K. Y.; Peyghambarian, N. *Nature* **1997**, 388, 845.
- (2) Kajzar, F.; Lee, K. S.; Jen, A. K. Y. *Adv. Polym. Sci.* **2003**, 161, 1.
- (3) Zyss, J. *Molecular Nonlinear Optics Materials Physics and Devices*; Academic Press: Orlando, FL, 1994.

- (4) Prasad, P. N.; Williams, D. J. *Introduction to Nonlinear Optical Effects in Molecules and Polymers*; John Wiley & Sons: New York, 1991.
- (5) Samyn, C.; Verbiest, T.; Persoons, A. *Macromol. Rapid Commun.* **2000**, *21*, 1.
- (6) Chaumel, F.; Jiang, H. W.; Kakkar, A. *Chem. Mater.* **2001**, *13*, 3389.
- (7) Verbiest, T.; Houbrechts, S.; Kauranen, M.; Clays, K.; Persoons, A. *J. Mater. Chem.* **1997**, *7*, 2175.
- (8) Zhang, C.; Ren, A. S.; Wang, F.; Zhu, J. S.; Dalton, L. R. *Chem. Mater.* **1999**, *11*, 1966.
- (9) He, M. Q.; Leslie, T. M.; Sinicropi, J. A. *Chem. Mater.* **2002**, *14*, 4662.
- (10) Yesodha, S. K.; Pillai, C. K. S.; Tsutsumi, N. *Prog. Polym. Sci.* **2004**, *29*, 45.
- (11) Moylan, C. R.; Twieg, R. J.; Lee, V. Y.; Swanson, S. A.; Betterton, K. M.; Miller, R. D. *J. Am. Chem. Soc.* **1993**, *115*, 12599.
- (12) Suresh, S.; Zengin, H.; Spraul, B. K.; Sassa, T.; Wada, T.; Smith, D. W. *Tetrahedron Lett.* **2005**, *46*, 3913.
- (13) Matsui, M.; Suzuki, M.; Hayashi, M.; Funabiki, K.; Ishigure, Y.; Doke, Y.; Shiozaki, H. *Bull. Chem. Soc. Jpn.* **2003**, *76*, 607.
- (14) Van den Broeck, K.; Verbiest, T.; Van Beylen, M.; Persoons, A.; Samyn, C. *Macromol. Chem. Phys.* **1999**, *200*, 2629.
- (15) Van den Broeck, K.; Verbiest, T.; Degryse, J.; Van Beylen, M.; Persoons, A.; Samyn, C. *Polymer* **2001**, *42*, 3315.
- (16) Sung, P. H.; Hsu, T. F.; Ding, Y. H.; Wu, A. Y. *Chem. Mater.* **1998**, *10*, 1642.
- (17) Cui, Y. J.; Qian, G. D.; Gao, J. K.; Chen, L. J.; Wang, Z. Y.; Wang, M. Q. *J. Phys. Chem. B* **2005**, *109*, 23295.
- (18) Gottlieb, H. E.; Kotlyar, V.; Nudelman, A. *J. Org. Chem.* **1997**, *62*, 7512.
- (19) Lebeau, B.; Brasselet, S.; Zyss, J.; Sanchez, C. *Chem. Mater.* **1997**, *9*, 1012.
- (20) Kwon, O.; Barlow, S.; Odom, S. A.; Beverina, L.; Thompson, N. J.; Zojer, E.; Bredas, J. L.; Marder, S. R. *J. Phys. Chem. A* **2005**, *109*, 9346.
- (21) Wang, X. M.; Zhou, Y. F.; Yu, W. T.; Wang, C.; Fang, Q.; Jiang, M. H.; Lei, H.; Wang, H. Z. *J. Mater. Chem.* **2000**, *10*, 2698.
- (22) Wurthner, F.; Yao, S.; Debaerdemaeker, T.; Wortmann, R. *J. Am. Chem. Soc.* **2002**, *124*, 9431.
- (23) Marder, S. R.; Beratan, D. N.; Cheng, L. T. *Science* **1991**, *252*, 103.
- (24) Palay, M. S.; Harris, J. M.; Looser, H.; Baumert, J. C.; Bjorklund, G. C.; Jundt, D.; Twieg, R. J. *J. Org. Chem.* **1989**, *54*, 3774.
- (25) Ermer, S.; Lovejoy, S. M.; Leung, D. S.; Warren, H. *Chem. Mater.* **1997**, *9*, 1437.
- (26) Oudar, J. L.; Chemla, D. S. *J. Chem. Phys.* **1977**, *66*, 2664.
- (27) Herman, W. N.; Hayden, L. M. *J. Opt. Soc. Am. B* **1995**, *12*, 416.
- (28) Maker, P. D.; Terhune, R. W.; Nisenhoff, M.; Savage, C. M. *Phys. Rev. Lett.* **1962**, *8*, 21.
- (29) Shuto, Y.; Amano, M. *J. Appl. Phys.* **1996**, *79*, 8.
- (30) Walsh, C. A.; Burland, D. M.; Lee, V. Y.; Miller, R. D.; Smith, B. A.; Twieg, R. J.; Volksen, W. *Macromolecules* **1993**, *26*, 3720.
- (31) Corriu, R. J. P.; Moreau, J. J. E.; Thepot, P.; Man, M. W. C. *Chem. Mater.* **1992**, *4*, 1217.
- (32) Katan, C.; Terenziani, F.; Mongin, O.; Werts, M. H. V.; Porres, L.; Pons, T.; Mertz, J.; Tretiak, S.; Blanchard-Desce, M. *J. Phys. Chem. A* **2005**, *109*, 3024.
- (33) Sanchez, C.; Lebeau, B.; Chaput, F.; Boilot, J. P. *Adv. Mater.* **2003**, *15*, 1969.
- (34) Briers, D.; Picard, I.; Verbiest, T.; Persoons, A.; Samyn, C. *Polymer* **2004**, *45*, 19.
- (35) Lee, K. S.; Kim, T. D.; Min, Y. H.; Yoon, C. S. *Synth. Met.* **2001**, *117*, 311.
- (36) Zhang, H. X.; Lu, D.; Fallahi, M. *Appl. Phys. Lett.* **2004**, *84*, 1064.